Structural revision of products resulting from the reaction of methylhydrazine with acridin-9-yl isothiocyanate due to unexpected acridinyl migration and further reactions

Karel D. Klika*[a], Eva Balentová[a,b], Juraj Bernát[b], Ján Imrich[b], Martina Vavrušová[b], Kalevi Pihlaja[a], Andreas Koch[c], Erich Kleinpeter[c], Alexandra Kelling,[c] and Uwe Schilde[c]

[a] Department of Chemistry, University of Turku, Vatselankatu 2, FIN-20014 Turku, Finland.
[b] Department of Organic Chemistry, P. J. Šafárik University, Moyzesova 11, SK-04167 Košice, The Slovak Republic. [c] Department of Chemistry, University of Potsdam, Am Neuen Palais 10, D-14415 Potsdam, Germany
*E-mail: klikakd@yahoo.co.uk*

Abstract

The reaction of methyl acridin-9-ylthiosemicarbazide under basic conditions with methyl bromoacetate resulted in a 1,3-thiazolin-4-one structure as provided by X-ray crystallography. The structure forced a re-evaluation of the reactant methyl acridin-9-ylthiosemicarbazide, originally thought to be 2-methyl 4-acridin-9-ylthiosemicarbazide based on synthetic expectations, but which when examined by X-ray crystallography was found to be in fact the isomeric 2-methyl 1-acridin-9-ylthiosemicarbazide resulting from rearrangement *via* a spiro form which it is in equilibrium with in solution. The product resulting from reaction with methyl iodide was also studied and the previously reported semicarbazide produced by reaction with MNO was re-examined. In both cases, the 1,2 isomer rather than the 2,4 isomer was found to be present based on the sign of the $^3J_{CH3,N11}$ coupling. Full characterization of the compounds was rendered by ^{1}H, ^{13}C, and ^{15}N solution-state NMR, and in the solid state, by both ^{13}C and ^{15}N NMR.

Keywords: NMR spectroscopy, X-ray crystallography, heterocycles, thiosemicarbazides, acridines, rearrangements

Introduction

Acridines have long been appreciated for their pharmaceutical applications[1–5] and, in particular, their promising oncological properties. Moreover, substantial biological effects can be anticipated for acridine intercalators connected to an additional heterocyclic moiety. As part of a study on (thio)semicarbazides wherein we wanted to compare structures with an acridinyl moiety

on the urea-type nitrogen (**A**)[6] against those with acridinyl on the terminal nitrogen of the carbazide (**B**),[7] we were confronted by the unexpected preparation of a 1,3-thiazolin-4-one structure from material purported to conform to structure **A**. This was part of a broad examination of acridine-[8–15] and anthracene-substituted[16,17] thioureas for the purposes of obtaining new and novel type structures concomitant with potential biological applications. The implication of this result was to force us to re-evaluate the structure of the starting thiosemicarbazide. One of the underlying themes in acridine-based work seems to be the pernicious desire of the N-10 atom to capture a proton[18] and thus drive the formation of spiro or iminyl structures for the acridine moiety (*i.e.* form 9,10-dihydro structures). It is through the former structure that isomerization can occur thus resulting in migration of the acridinyl unit from one end to the other of the thiosemicarbazide moiety. As a result, whereas previously[6] we considered the solution equilibrium to be between 4-(9,10-dihydroacridin-9-yliden)-2-methylthiosemicarbazide (**1**) and 2′-methyl spiro[dihydroacridinyl-9(10*H*),5′-1′,2′,4′-triazolidine]-3′-thione (**2**), we are now compelled to modify this to the following system outlined in Scheme 1. Reviews of this type of ring–open-chain tautomerism are present in the literature.[19]

R, R' = H, alkyl, aryl
X = O, S

A   **B**

4   **1:** R = methyl   **2**   **3**
                        5: R = H
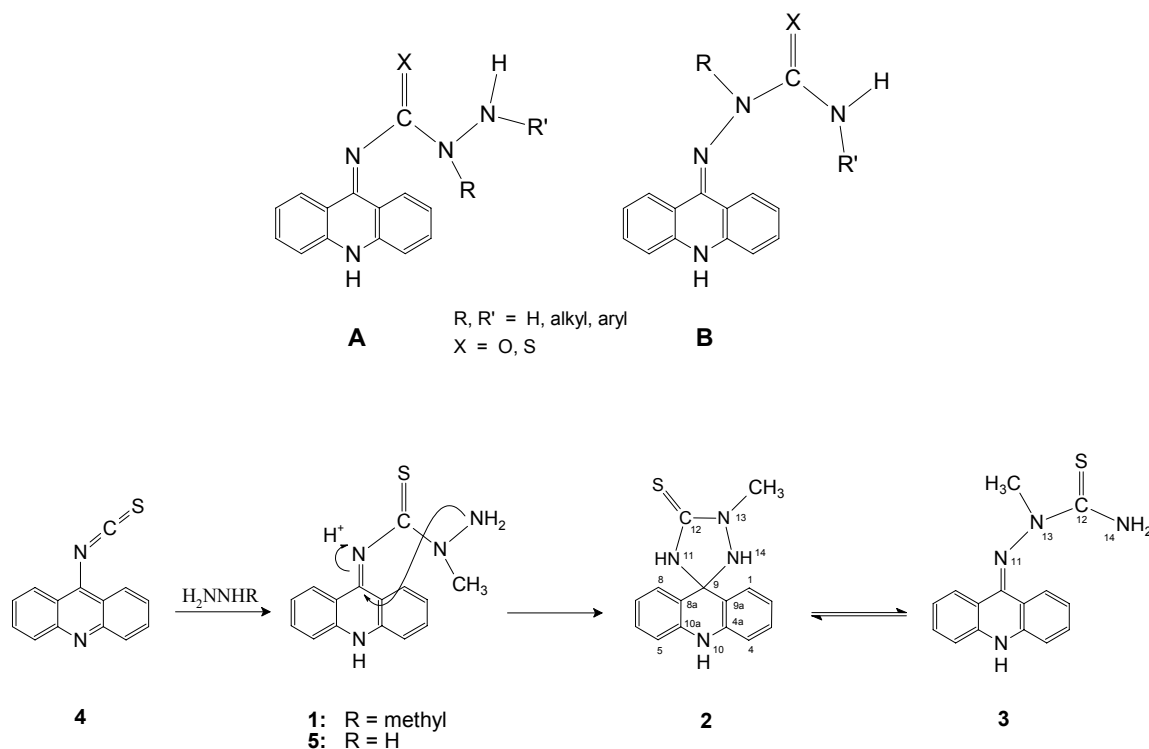
Scheme 1. The reaction sequence giving rise to 1-(9,10-dihydroacridin-9-yliden)-2-methylthiosemicarbazide (**3**).

The solution equilibrium was formerly thought[6] to be between the open-chain form **1** and the spiro form **2** but it has now been determined that the spiro form **2** is in equilibrium with the

open-chain form **3**. For convenience, the carbonyl carbon retains its designation as C-12 and the methyl-bearing nitrogen its designation as N-13 in the 1,2-substituted regioisomers.

Results and Discussion

The reaction of the material–present as a mixture of open-chain and spiro forms[6]–resulting from the addition of methylhydrazine to acridin-9-yl isothiocyanate (**4**) with methyl bromoacetate yielded the product 2-[2-(9,10-dihydroacridin-9-yliden)-1-methylhydrazino]-4,5-dihydro-1,3-thiazol-4-one (**6**) whose structure depicted in Figure 1 was determined by X-ray crystallographic analysis. The ^{1}H, ^{13}C, and ^{15}N chemical shifts of **6** together with all other compounds discussed in this work are compiled in Tables 1 and 2. Signal assignments were accomplished by the application of the usual combination of ^{1}H, ^{13}C, and ^{15}N chemical shifts assisted by DEPT, NOE difference, and ^{15}N INEPT 1-D experiments and DQF COSY, ^{13}C–{^{1}H}-CHDEC, ^{1}H–{^{13}C}-HSQC PMG, ^{1}H–{^{13}C}- and ^{1}H–{^{15}N}-HMBC, and ^{1}H–{^{15}N}-HSQC 2-D experiments. In the ^{1}H NMR, upon lowering the temperature to –25 °C, the rapid exchange of the ring methylene protons in **6** was slowed sufficiently to observe the symmetric site interconversion. This slow interconversion of the methylene protons can be understood on the basis of the rigid segment present in the five-membered ring (C=N–C=O) thus allowing the unique movement of the methylene group to be realized. Examination of compound **6** in the solid state by ^{13}C and ^{15}N NMR (Table 1) provided only one set of signals with close similarities to the solution-state ^{13}C and ^{15}N chemical shifts and consistent multiplicities of the nitrogens with their assignments.
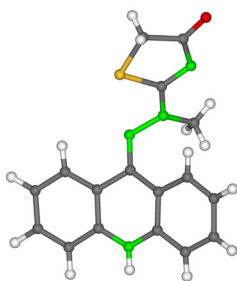

Figure 1. The structure of **6** provided by X-ray crystallographic analysis.

   One of the great difficulties in this work was to obtain crystals of **6** suitable for X-ray analysis and we were consistently thwarted by the persistent failure to obtain suitable X-ray quality crystals, or even clearly crystalline material for that matter as, mostly, a glassy-type melt was all that could be obtained. Conventional crystallization using a variety of solvents was unsuccessful, as were mixed solvent systems, sublimation, and deep freeze–slow evaporation attempts. It is possible that tautomeric equilibrium, *e.g.* the labile proton can translate from N-10

to N-11, was responsible for precluding crystallization and as an attempt to alleviate this, crystallization in an electric field was tried. Interestingly, electric or magnetic fields have been well examined with regards to their application to crystallization in the inorganic realm but seem to be quite limited with respect to organic systems, the ubiquitous presence of liquid crystals notwithstanding. The particular cases reported recently for organic systems[21] are more aimed at perturbation of the crystalline structure itself than obtaining crystals *per se*. Though it must be noted that in consideration of this context the idea extends back[22] to Pasteur who applied magnetic fields in the vain hope[23] of effecting the preferential crystallization of enantiomers from racemic solutions. The electric field crystallization as performed did provide crystalline samples, although the initially formed material was not of sufficient quality for X-ray analysis as it comprised of star-burst clumps of needles or wafer-like crystals. However, repeated, partial recrystallizations from methanol (*i.e.* the crystals were only partly resolved) of the originally obtained material (from DMF) finally yielded X-ray crystallographic-grade single crystals. Whether the electric field was required for the repeated recrystallizations was not evaluated, however, the isolation of clear crystalline material in itself was hitherto not accomplished except in the presence of the electric field.

The course of the reaction (see Scheme 2) to provide this structure is easily anticipated from either **2** or **3**, the sulfur (as thiol) can displace bromide from methyl bromoacetate followed by spiro ring opening in the case of **2** and then attack of the nitrogen in the urea-type position (imine in both cases) to displace methoxide to form the thiazolinone ring. The quintessential question is then whether it is the spiro form **2** (present[6] in DMSO solution as a minor interconverting species with a major open-chain form, *ca.* 96:4) or the open-chain 1,2-substituted regioisomer **3** that undergoes the reaction with methyl bromoacetate. However, even though the spiro form **2** can react to yield **6**, it was hence considered necessary to confirm both the solid-state structure and the solution-state structure of the major species of the equilibrium as it calls into question the structure assumed to be the 2,4-substituted regioisomer. For this reason, crystals were grown of the starting material **3** and subjected to X-ray crystallographic analysis. The result is depicted in Figure 2 where clearly it is the 1,2-substituted regioisomer that has crystallized. It is worth noting that it was the inability to resolve the structure of **6**, finally determined by X-ray crystallographic analysis, that led to the realization that perhaps a structural revision, or at least a confirmation of the structure of the starting material, was required as the possibility of ring opening to provide the regioisomeric 1,2-substituted thiosemicarbazides was not considered in the previous study. It was also necessary to confirm the solution-state structure as reaction back to the 2,4-substituted regioisomer (**1**) is conceivable in solution.

**Table 1.** ^{13}C and ^{15}N NMR[a] chemical shifts (δ in ppm)

struct	C-1	C-2	C-3	C-4	C-4a	C-5	C-6	C-7	C-8	C-8a	C-9	C-9a	N-10	C-10a	N-11	C-12	N-13	N-14	others
2	126.92	119.69	129.06	113.97	138.04	113.97	129.06	119.69	126.92	119.10	74.22	119.10	−282.0	138.04	−245.7	177.40	−246.8	−243.1	34.40 (NMe)
3[b]	127.17	120.51	132.55	117.21	140.36	115.81	131.58	121.03	126.23	117.93	155.38	113.48	−266.7	138.15	−106.6	177.84	−234.2	−273.3	39.28 (NMe)
											solid-state NMR:		−265.7	–	−99.2	–	−231.1	−272.2	–
5[b]	127.31	119.39	131.13	116.53	141.02	115.02	130.11	120.78	125.44	118.94	141.68	114.13	–	138.41	–	177.72	–	–	39.06 (NMe),
6	126.62	120.97	133.04	117.67	140.28	116.31	132.25	121.63	125.15	116.97	157.32	112.53	−264.0	138.08	−93.3	180.53	−233.2	–	39.84 (CH$_3$), 186.11 (C=O)
											solid-state NMR:		−262.6	–	−101.8	–	−231.3	−154.1	–
7[b]	128.32	119.59	131.75	116.59	140.67	115.58	130.79	120.85	125.79	118.83	151.37	114.49	−270.3	138.30	−78.3	160.20	−255.8	−301.6	34.87 (NMe)
8	128.07	119.53	131.71	116.61	140.51	115.61	130.79	120.88	125.18	118.81	151.13	114.33	−265.3	138.20	−94.6	166.33	−261.4	–	13.30 (SMe), 37.93 (NMe)
											solid-state NMR:		−248.7	–	−89.6	–	−266.2	−195.1	–
9	127.44	119.28	128.06	113.45	137.64	113.45	128.06	119.28	127.44	122.24	84.51	122.24	−282.5	137.64	–	164.67	–	−235.32	14.45 (SMe), 38.77 (NMe)
10	126.18	121.26	133.30	117.82	140.22	116.27	132.43	121.6	125.6	116.8	157.73	112.22	−262.5	138.02	−68.2[c]	166.0	–	−231.7	14.48 (SMe), 39.80 (NMe)
											solid-state NMR:[d]		−83.4, −106.6, −231.9, −235.3, −252.0, −263.1, −268.8, −279.1						

[a] In DMSO-d_6 at 25 °C for solution-state spectra, ambient temperature for solid-state spectra; values are given to only one decimal place for very broad signals or those measured indirectly; ^{13}C referenced internally to TMS (0 ppm); ^{15}N referenced externally to CH_3NO_2 (0 ppm) for solution-state spectra and internally to NH_4Cl (−343 ppm relative to liquid CH_3NO_2 at 0 ppm) for solid-state spectra. [c] Chemical shift questionable. [d] All observed shifts.

Table 2. ¹H NMR data[a] (δ in ppm; J in Hz)

struct	H-1	H-2	H-3	H-4	H-5	H-6	H-7	H-8	H-10	H-14	others
2	7.58	7.02	7.35	7.08	7.08	7.35	7.02	7.58	9.68	6.00 b	3.15 (NMe), 9.49 (H-11)
3[b]	8.07	7.10	7.59	7.38	7.30	7.55	7.14	8.47	11.12	7.07, 7.57	3.29 (NMe)
3, J[a,b]	$J_{H1,H2}=8.5$, $J_{H1,H3}=-1.4$, $J_{H1,H4}=0.5$, $J_{H1,H10}=0.5$, $J_{H2,H3}=7.0$, $J_{H3,H4}=-1.3$, $J_{H3,H4}=8.4$, $J_{H5,H6}=8.3$, $J_{H5,H7}=-1.2$, $J_{H5,H8}=0.5$, $J_{H6,H7}=7.0$, $J_{H6,H8}=-1.5$, $J_{H7,H8}=8.3$, $J_{H8,H10}=0.5$										
5[b]	8.22	7.08	7.48	7.25	7.14	7.40	7.02	8.39	10.48	7.80, 8.15	10.01 (b, H-13)
6	8.02	7.19	7.67	7.48	7.41	7.65	7.23	8.40 dd	11.52	–	3.37 (NMe), 3.90 (SCH₂)
6, J[b]	$J_{H1,H2}=8.6$, $J_{H1,H3}=-1.3$, $J_{H1,H4}=0.5$, $J_{H2,H3}=6.9$, $J_{H2,H4}=-1.3$, $J_{H3,H4}=8.4$, $J_{H5,H6}=8.3$, $J_{H5,H7}=-1.1$, $J_{H5,H8}=0.5$, $J_{H6,H7}=7.0$, $J_{H6,H8}=-1.5$, $J_{H7,H8}=8.3$; at $-25\,°C$, $J_{gem}=-17.45$										
7[b]	8.45	7.06	7.50	7.31	7.25	7.49	7.09	8.43, dd	10.75	6.35s	2.86 (NMe)
7, J[a,b]	$J_{H1,H2}=8.4$, $J_{H1,H3}=-1.4$, $J_{H1,H4}=0.6$, $J_{H2,H3}=7.0$, $J_{H2,H4}=-1.2$, $J_{H3,H4}=8.3$, $J_{H5,H6}=8.2$, $J_{H5,H7}=-1.1$, $J_{H5,H8}=0.6$, $J_{H6,H7}=7.0$, $J_{H6,H8}=-1.5$, $J_{H7,H8}=8.2$										
8	8.42	7.04	7.50	7.29	7.23	7.47	7.08	8.27	10.78	7.37 b	2.22 (SMe), 2.99 (NMe)
9	7.29	6.88	7.20	6.92	6.92	7.20	6.88	7.29	9.38	5.28 b	2.54 (SMe), 2.79 (NMe)
10	7.90 dd	7.23	7.73	7.55	7.46	7.70	7.26	8.45 dd	11.68	8.83 b	2.70 (b, SMe), 3.38 (b, NMe)
10, J[b]	$J_{H1,H2}=8.5$, $J_{H1,H3}=-1.4$, $J_{H1,H4}=0.5$, $J_{H2,H3}=7.0$, $J_{H3,H4}=-1.3$, $J_{H3,H4}=8.4$, $J_{H5,H6}=8.3$, $J_{H5,H7}=-1.2$, $J_{H5,H8}=0.5$, $J_{H6,H7}=7.0$, $J_{H6,H8}=-1.5$, $J_{H7,H8}=8.3$										

[a] In DMSO-d₆ at 25 °C; shifts referenced internally to TMS (0 ppm). [b] All aromatic ¹H signals present as ddd (except where noted) and Js extracted using Perch simulation software[20] with signs assumed on the basis of ^{odd}J = +ve and ^{even}J = −ve; all other signals were present as singlets. Legend: b, broad; (d)dd, (doublet of) doublet of doublets.
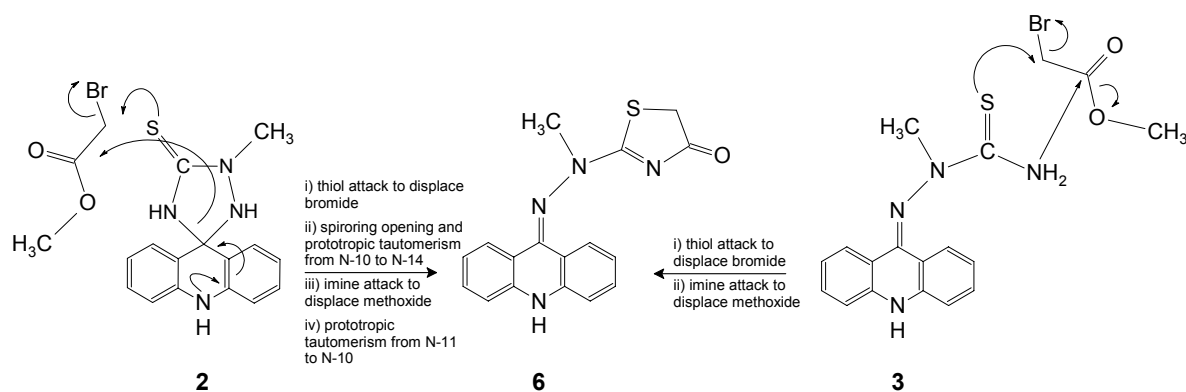
Scheme 2. The possible reaction sequences shown in compacted form for the spiro form **2** and the open-chain 1,2-substituted regioisomer **3** with methyl bromoacetate leading to the product **6**.
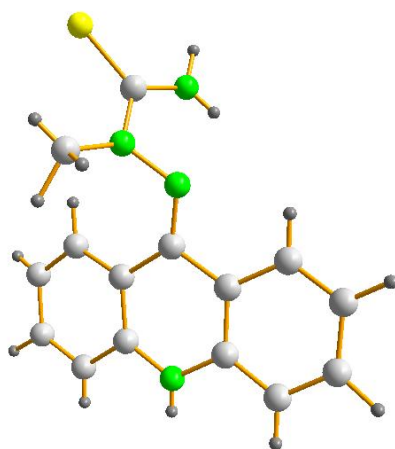

Figure 2. The X-ray crystallographic structure of **3**.

Differentiation of the 2,4- and 1,2-substituted regioisomers (**1** and **3**, respectively) in solution is far from straightforward and potential long-range couplings to effect such a distinction are portrayed in Figure 3, with the full gamut of possibilities succinctly presented in Table 3.
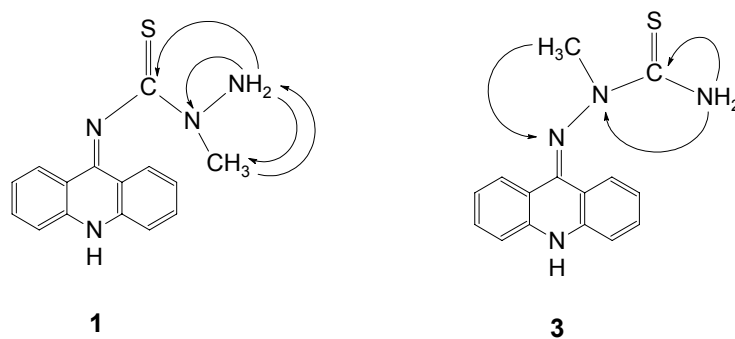
Figure 3. Viable long-range ^1H–^{15}N and ^1H–^{13}C NMR correlations that can potentially distinguish between **1** and **3**.

Table 3. Potential long-range correlations (in terms of the number of bonds for the **1/3** structures) between the protons of the thiosemicarbazide and the N and C atoms contained within

Proton	N–CH$_3$	NH$_2$/CH$_3$	=N	C=S(O)
CH_3	2/2	3/4	4/3	3/3
NH_2	2/3	3/4	4/4	3/2

Obviously entries with the same values for each structure are indeterminate. Entries [1,2] and [1,3] suffer from the possibility of extended long-range coupling, *i.e.* the pernicious property of a proton to display couplings to nitrogen over more than three bonds,[24–28] and therefore the actual presence of such correlations *is not unequivocal*. Entry [2,2] is only informative if it is present and thereby indicating structure **1** (*i.e.* a lack of observation is meaningless). Finally, the mere presence of correlations relating to entries [2,1] and [2,4] does not effect any distinction. The pivotal data to effect the required distinction is the sign of the coupling giving rise to the correlations as this can allow one to distinguish between correlations over 2 or 3 bonds or 3 or 4 bonds. The analysis follows the methodology and reasoning outlined by Roslund *et al.*[29] regarding the determination of the signs of $^nJ_{H,X}$ as appropriate for interactions involving two spins both possessing positive γ values or for interactions involving one $+\gamma$ nucleus and one $-\gamma$ nucleus. This methodology–essentially using 2-D HMQC spectra–is applicable to three ^{1}H–^{15}N couplings (entries [1,2], [1,3], and [2,1]) and two ^{1}H–^{13}C couplings (entries [2,2] and [2,4]) in these systems (and with the proviso that the observed coupling is large).

Of the five potential correlations to effect distinction between the two regioisomers, only one was observed, mainly due to the breadth of the NH$_2$ proton signals. The one important correlation that was observed, the one between the NCH$_3$ protons and N-11 (entry [1,3]), was negative in sign as appropriate for a three-bond coupling involving one $+\gamma$ nucleus and one $-\gamma$ nucleus. By comparison, the two-bond coupling between the methyl protons and N-13 (entry [1,1]) was of opposite sign (positive) in accordance with expectations.

Compound 4-(9,10-dihydroacridin-9-yliden)thiosemicarbazide (**5**),[6] which does not bear a methyl substituent, presumably undergoes the same migration reaction based on the chemical shifts after due allowance for the methyl group lacking. Regarding the ^{1}H NMR spectra of both **3** and **5**, it is, quite naturally, the restricted rotation about the thioamide-type bond that is responsible for the distinctiveness of the NH$_2$ protons, formerly attributed to internal hydrogen bonding. Compound **3** was also examined in the solid state by ^{13}C and ^{15}N NMR (Table 1) wherein it was ascertained that only one species was present as implied by the one set of signals, but it is plausible given the solution-state equilibrium that the content of **2** simply lies below the level of detection. (Compound **2** is readily identifiable by the distinct presence of its sp^3-hybridized C-9 atom at *ca.* 74 ppm.) It is inferred that the predominant species adopted in solution, **3**, is retained in the solid state based on the observed similarity of the ^{13}C and ^{15}N chemical shifts. The multiplicities of the nitrogens in **3** were, moreover, consistent with their assignments based on equating NH with carbon methine behavior and terminal NH$_2$ with carbon methyl behavior.

In a previous study,[6] **3** was treated with mesitylnitrile oxide (MNO) to effect an S → O transmutation (Scheme 3) wherein no change to the substitution pattern was considered. The product of this reaction, 1-(9,10-dihydroacridin-9-yliden)-2- methylsemicarbazide (**7**), was therefore also scrutinized by the same methodology leading to the conclusion that it did in fact retain the same substitution pattern as **3**, *viz.* it was a 1,2-substituted semicarbazide and not the 2,4-substituted regioisomer as previously reported. The NH_2 proton signal in this case was relatively sharp, though no correlation was observed to the methyl carbon, the correlation to N-13 was indeterminate in terms of sign, and the coupling to C-12 was small and therefore not valid for structure determination based on its sign. The important correlation between the NCH_3 protons and N-11 was negative, in accordance with a three-bond coupling for ^1H and ^{15}N. The two-bond coupling between the methyl protons and N-13 was, by comparison, positive.

The treatment of **2/3** with CH_3I and base was found to also provide an equilibrium of open-chain *S*-methyl 1-(9,10-dihydroacridin-9-yliden)-2- methyl isothiosemicarbazide (**8**) and spiro 2′-methyl-3′-methylthiospiro[dihydroacridinyl-9(10*H*),5′-1′,2′-dihydro-1′,2′,4′-triazole] (**9**) forms in an 85:15 ratio, respectively (Scheme 4).
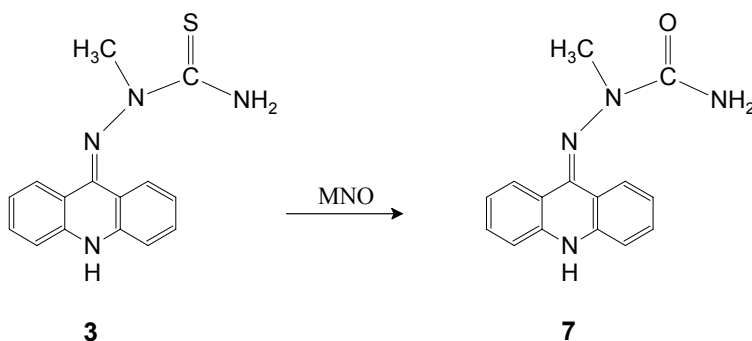

Scheme 3. The structure of **7** retained the 1,2-substitution of **3** after reaction based on the negative sign of the long-range coupling between the methyl protons and N-11.
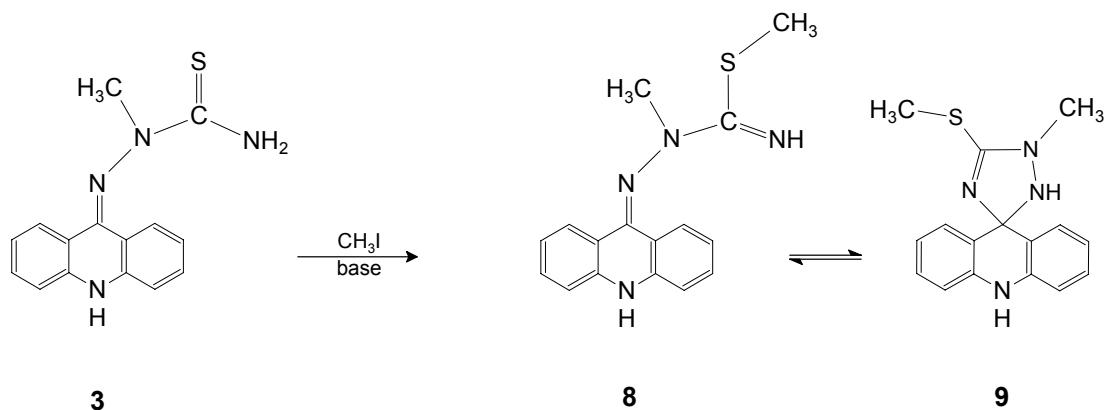
Scheme 4. The reaction of **3** with methyl iodide and base yielded an equilibrium of open-chain **8** and spiro **9** forms in a ratio of 85:15, respectively. The 1,2-substitution pattern of **8** was confirmed by the negative sign of the coupling between the methyl protons and N-11.

Both products are clearly S-methylated based on the shielding of the introduced methyl group and a labile H resides on N-10 based on NOEs from H-10 to H-4 and H-5, which amounted to *ca.* 20% each, and on correlations observed from H-10 to both C-8a and C-9a. The other labile H on N-14 in structure **8** was not explicitly observed, though the presence of a broad underlying signal in the aromatic region was implicated by integration. The structure of **9** was quite evident based on the chemical shift of C-9 (84.5 ppm) together with the equivalence of the off-central axis nuclei of the acridine moiety (the outer rings). The breadth of the H-14 signal in **8** precluded correlations to it and determination the sign of the coupling (negative) between the methyl protons and N-11 again inferred that **8** is 1,2-substituted. Examination of the sample of **8** and **9** in the solid state by ^{13}C and ^{15}N NMR (Table 1) revealed that in addition to a major predominate form, consistent with **8** based on the observed ^{13}C and ^{15}N chemical shifts, two (*ca.* 10 and 5%) or possibly more species were also present. The 5% species clearly alluded to the spiro form **9** based on a signal for C-9 resonating in the appropriate range.

The protonated product, *S*-methyl 1-(9,10-dihydroacridin-9-yliden)-2-methyl isothiosemicarbazide hydroiodide (**10**), was also examined, *i.e.* the product obtained without base treatment (Scheme 5). An equilibrium between open-chain and spiro forms in this instance, however, was not observed. In addition to the observation of a single labile proton at 11.68 ppm (H-10), a two-proton singlet was also observed for the H-14 atoms at 8.83 ppm. Low temperature measurements (−75 °C) indicated that the spectrum observed at 25 °C is actually a time-averaged confluence of two conformers. Since it was the signals of C-12 and the S-methyl protons (and also C-8?) that deconvoluted into separate signals, restricted rotation must be occurring about the C$_{12}$−S bond to give rise to *E*- and *Z*-type conformers which are in fast equilibrium at room temperature. NOE measurements at −75 °C, unfortunately, failed to provide assignment of the two sets of signals. But it is the existence of this equilibrium which conveys a strong indication that there must be appreciable double bond character present in the C$_{12}$−S bond of **10**.
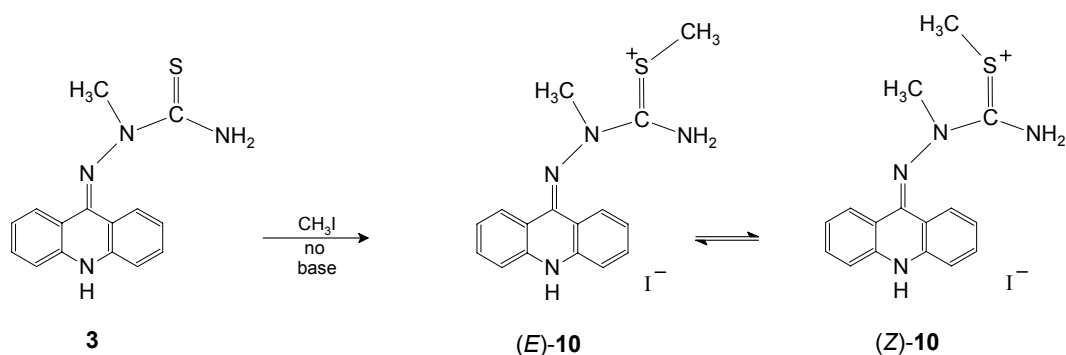
Scheme 5. Methylation of **3** without base yielded only one set of NMR signals for the product at 25 °C. However, this was shown to be a mixture of interconverting *E*- and *Z*-type conformers upon lowering the temperature to −75 °C and clearly therefore there must be some double bond character to the S−C$_{12}$ bond to explain this observation.

Examination of *S*-methyl 1-(9,10-dihydroacridin-9-yliden)-2-methylisothiosemi- carbazide hydroiodide (**10**) in the solid state by ^{13}C and ^{15}N NMR (Table 1) revealed a very complex state with at least two, possibly three, significant species present. One of these is very different to the solution-state species but it is not the spiro form as evidenced by the absence of a signal in the 60−90 ppm range. The system, however, was beyond disentanglement with respect to structural assignment.

One final aspect of the previous report[6] concerns the reaction of **2/3** with acetone (Scheme 6) to yield a product identical with that produced by the reaction of acridin-9-yl isothiocyanate (**4**) with acetone 2-methyl hydrazone to provide 4-(9,10-dihydroacridin-9-ylidene)-1-isopropylidene-2-methylthiosemicarbazone (**11**) and a cyclic isomer 4-(acridin-9-yl)-2,5,5-trimethyl-1,2,4-triazolane-3-thione (**12**). The course of this reaction is reaffirmed despite the structural revision of **1** to **3**. The reaction can occur through the spiro form **2** and reaction all the way back to **1** is unnecessary to rationalize the product, which ironically represents a 2,4-substituted regioisomeric structure. The cyclic structures of the previous study[6] certainly remain valid, as indeed these are the intermediates by which the isomers rearrange. The reaction to yield **6** also shows that the imine nitrogen can participate as a nucleophile if the amine nitrogen is blocked for these systems.
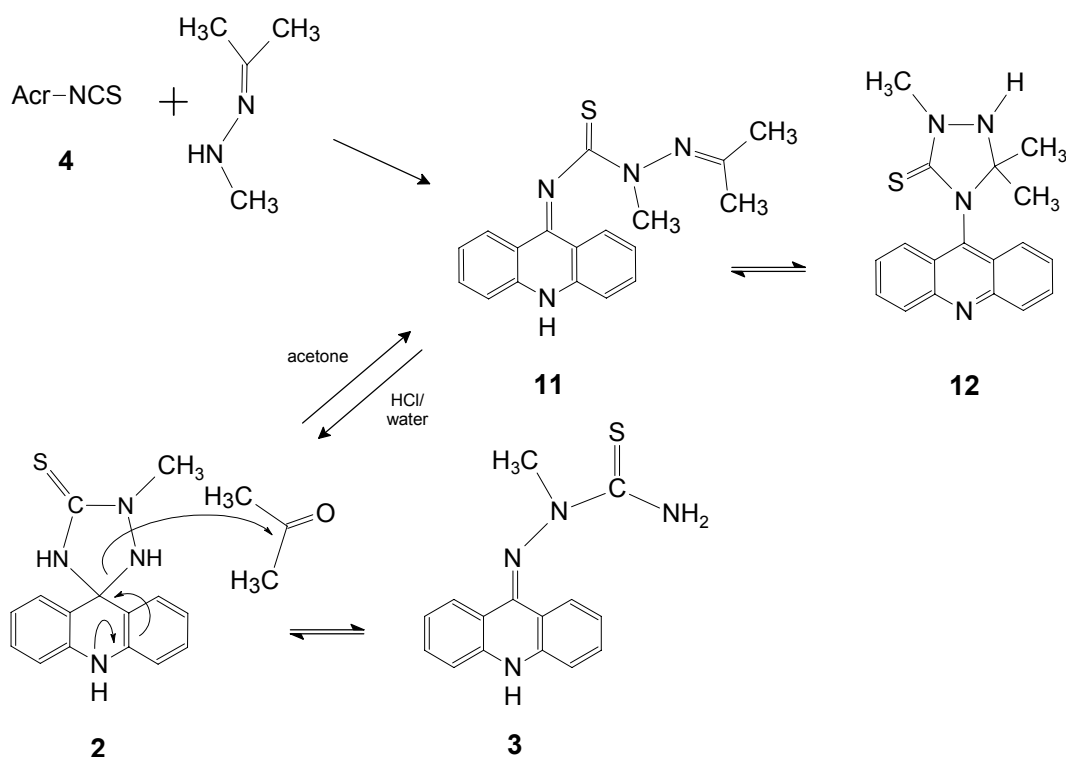
Scheme 6. It had previously been reported[6] that **3** reacts with acetone to yield **11** which is in equilibrium with **12**, this reaction stands but evidently the reaction must proceed through the spiro form **2** to yield the structure shown.

Experimental Section

General Procedures. IR spectra were recorded on a Specord M80 spectrophotometer (Zeiss, Jena) as KBr discs. ESI-MS analysis was performed using a Perkin–Elmer Sciex API-365 triple quadrupole mass spectrometer equipped with a pneumatically-assisted ion spray interface with the needle voltage set at +5,000 V (–4,400 V), the orifice plate voltage at +35 V (–35 V) and the ring voltage at +220 V (–200 V) for positive (negative) ion measurements. The nebulizer gas (purified air) flow was set at position 9 and that for the curtain gas (N_2) at position 12. The heated nitrogen gas temperature was set at 300 °C and the gas flow rate at 7 L min^{-1}. Masses were scanned from m/z 100 to 3,000 in 0.3 amu steps. Ions in inverted commas are hypothetical; the net loss of fragments, *i.e.* ambiguity regarding the precise fragmentation, is indicated by the placement of such within parallel lines. Elemental analysis was performed using a Perkin–Elmer CHN 2400 analyzer. Melting points were determined on a Boetius instrument and are uncorrected.

Solution-state NMR spectra were acquired using a JEOL Alpha 500 NMR spectrometer operating at 500 MHz for ^1H, 126 MHz for ^{13}C, and 51 MHz for ^{15}N. NOE difference measurements were acquired using saturation times of 6 s at a reduced level of resolution (3.9 Hz pt^{-1}). Phase-sensitive DQF-COSY, CHDEC (CHSHFT with f1 homonuclear decoupling), and HSQC PMG[29] and magnitude mode HMBC BIRD spectra were acquired with spectral widths and resolution appropriately optimized from the 1-D spectra. Both HSQC and HMBC spectra utilized a $^1J_{HC}$ coupling of 145 Hz, whilst the HMBC correlations were optimized for a long-range $^nJ_{HC}$ coupling of *ca.* 8 Hz. ^{15}N shifts were generally acquired indirectly from the f1 dimension of FGHSQC or FGHMBC experiments where both HSQC and HMBC spectra utilized a $^1J_{HN}$ coupling of 90 Hz whilst the HMBC correlations were optimized for a long-range $^nJ_{HN}$ coupling of 8 Hz. The f1 windows and resolution were set according to judgment based on previous experience and affordability. The determination of the signs of the long-range couplings were carried out in accordance with the protocol set out in Roslund *et al.*[29] Refocused-INEPT experiments permitted direct observation of ^{15}N nuclei where the final two delays were set to either 1/(4*J*) or 3/(4*J*). Further details are available in reference.[7]

Solid-state ^{13}C and ^{15}N CP/MAS NMR spectra were acquired on a Bruker Avance NMR spectrometer without lock at ambient temperature in a field of 9.4 T operating at 100 MHz for ^{13}C and 40 MHz for ^{15}N using standard cross polarization (contact times 15 and 25 ms, respectively; post-acquisition delay 10 s) with TPPM decoupling[31] (0/20º) at 12 and 9 kHz rotor speeds, respectively, in 4 mm ZrO_2 rotors. Teflon spacers were used in cases of limited sample amount to contain the material within the sampling volume (*ca.* 50 μL). 1 k data points were collected for each FID (acquisition time = 6.4 ms) which were processed by zero-filling to 32 k and applying a line broadening of 25–100 Hz. Ammonium chloride (5–10%) was used as an internal reference for ^{15}N spectra (–343 ppm relative to liquid nitromethane at 0 ppm) and ^{15}N atom multiplicities were evaluated based on NQS[32] (dephase/rephase time = 45 μs) and CPPI[33,34]

(polarization inversion time = 40 μs) experiments. [13]C chemical shifts were not internally referenced and are therefore not reported.

X-ray studies were performed on an IPDS-2 diffractometer (Stoe) using graphite-monochromated Mo-K$_\alpha$ radiation (λ = 0.71073 Å) at 210 K. Structure solution was by direct methods (SHELXS-97)[35] and full-matrix refinement against F^2 (SHELXL-97).[36] Non-hydrogen atoms were refined with anisotropic temperature factors. Crystallographic information files are available as Supplementary Information. Crystallographic data for the structures have been deposited with the Cambridge Crystallographic Data Centre. These data can be obtained free of charge *via* http://www.ccdc.cam.ac.uk/data_request/cif on quoting the deposition numbers CCDC-632863 (**6**) and CCDC-632864 (**3**).

Compounds 2/3, 5, and 7. The synthetic preparation for compounds **2/3**, **5**, and **7** have been reported.[6] Crystals of **3** suitable for X-ray analysis were obtained by the slow evaporation of a methanol solution to yield monoclinic crystals belonging to the *C*2/*c* space group. Molecular formula, $C_{15}H_{14}N_4S \cdot CH_3OH$; M = 314.40; Z = 8; a = 13.0477(19) Å; b = 21.262(3) Å; c = 12.0046(19) Å; β = 106.961(12)°; V = 3185.4(8) Å^3; D_x = 1.311 g·cm^{-3}; 2799 unique data, ($2\theta_{max}$ = 50°), 1931 with $I > 2.0\sigma(I)$; R = 4.06; Rw = 0.0949; S = 0.897. Full crystallographic details are available in the Supplementary Information.

2-[2-(9,10-Dihydroacridin-9-yliden)-1-methylhydrazino]-4,5-dihydro-1,3-thiazol-4-one (6). To a solution of **2/3**[6] (0.5 g, 1.7 mmol) in methanol (15 mL), methyl bromoacetate (0.172 mL 1.87 mmol) was added dropwise followed by sodium methoxide (0.1 g, 1.87 mmol). The mixture was then allowed to stir under an atmosphere of nitrogen at room temperature for 5 h. The precipitate was collected by filtration, washed with ether, and then recrystallized from ethanol to afford **6** as a yellow powder. Yield 57%; mp 251–253 ºC (ethanol); Found: C, 62.94; H, 4.13; N, 16.98. $C_{17}H_{14}N_4OS$ requires C, 63.33; H, 4.38; N, 17.38%; ν_{max} (KBr)/cm^{-1} 1660, 1620, 1540, 1493, 1466, 1347, 1268, 1245, 743; *m/z* (+ve): 989 (3M + Na$^+$, 1.7%), 967 (3M + H$^+$, 0.4), 667 (2M + Na$^+$, 41), 645 (2M + H$^+$, 2.9), 345 (M + Na$^+$, 100), 323 (M + H$^+$, 69), 249 (M$^+$ + H – ⌐CH$_3$, SH⌐, 4.7), 195/194/193 ($C_{13}N_2H_{11-9}$, 9.5/26/32); *m/z* (–ve): 643 (2M – H$^+$, 4.1), 321 (M – H$^+$, 100). The solvents tried (repeatedly) under various conditions including low temperature, slow evaporation, *etc.* for the crystallization of **1** included: acetonitrile, DMF, chloroform, acetone, dichloromethane, methanol, DMSO, nitromethane, and formamide as well as combinations thereof. Sublimation was also found to be unsuccessful. For crystallizations in an electric field, solutions in vials (7.2 mL in volume) were placed in an electric field emanating from brass plates (7 × 4 cm) spaced 2 cm apart and charged to 3 kV. Solvents tried included acetonitrile, DMF, chloroform, and methanol and crystallization was allowed to proceed by the slow evaporation of the solvent. Following the collection of crystals from DMF, repeated partial re-solvation of the material using methanol (maintained in an electric field) afforded a final crop of monoclinic crystals belonging to the *P*2$_1$/*c* space group. Molecular formula, $C_{17}H_{14}N_4OS$; M = 322.38; Z = 4; a = 5.1320(9) Å; b = 17.205(2) Å; c = 17.042(3) Å; β = 90.183(15)°; V = 1504.8(4) Å^3; D_x = 1.423 g·cm^{-3}; 2557 unique data, ($2\theta_{max}$ = 50°), 1316 with $I > 2.0\sigma(I)$; R =

4.51; Rw = 0.0485; S = 0.804. Full crystallographic details are available in the Supplementary Information.

_S_-Methyl 1-(9,10-dihydroacridin-9-yliden)-2- methyl isothiosemicarbazide (8) and 2´-methyl-3´-methylthiospiro[dihydroacridinyl-9(10_H_),5´-1´,2´-dihydro-1´,2´,4´-triazole] (9). To a stirred suspension containing **2/3**[6] (0.423 g, 1.5 mmol) and anhydrous K_2CO_3 (0.31 g, 2.25 mmol) in dry acetonitrile (10 mL) at room temperature, CH_3I (0.212 g, 0.093 mL, 1.5 mmol) was added dropwise and the mixture left to stir for 6 h at room temperature. The resulting precipitate was collected by filtration, washed with ether, dried, and then recrystallized from ethanol to provide a mixture of **8** and **9** (solution equilibrium by ^{1}H NMR 85:15). Yield 68%; mp 210–214 °C (ethanol); Found: C, 65.05; H, 5.80; N, 19.21. $C_{16}H_{16}N_4S$ requires C, 64.84; H, 5.44; N, 18.90%; v_{max} (KBr)/cm^{-1} 1628, 1554, 1473, 1408, 1362, 1256, 1157, 1117, 1042, 955, 748, 651; m/z (+ve): 297 (M + H$^+$, 100%), 249 (M + H$^+$ – $|CH_3, SH|$, 92), 234 (M + H$^+$ – $|2 \times CH_3, SH|$, 59), 195/194/193/192 ($C_{13}N_2H_{11-8}$, 73/100/92/29); m/z (–ve): 281 ("M$^-$" – $|CH_3|$, 100).

_S_-Methyl 1-(9,10-dihydroacridin-9-yliden)-2-methyl isothiosemicarbazide hydroiodide (10). To a solution of **2/3**[6] (0.423 g, 1.5 mmol) in dry acetonitrile (10 mL), CH_3I (0.212 g, 0.093 mL, 1.5 mmol) was added slowly and the mixture left to stir for 8 h at room temperature. The precipitate was collected by filtration, washed with ether, dried, and then recrystallized from diethyl ether affording the product **10**. Yield 65%; mp 187–189 °C (diethyl ether); Found: C, 45.63; H, 4.19; N, 12.92. $C_{16}H_{17}IN_4S$ requires C, 45.29; H, 4.04; N, 13.20%; m/z (+ve): 297 (M + H$^+$, 100%), 249 (M + H$^+$ – $|CH_3, SH|$, 71), 196/195/194/193 ($C_{13}N_2H_{12-9}$, 29/52/53/46); m/z (–ve): 281 ("M$^-$" – $|CH_3|$, 100), 194 ($C_{13}N_2H_{10}$, 25).

Acknowledgements

Supplementary Information Available

Crystallographic information files (CIF) for **3** and **6**.

References

1. Denny, W. A. *Anticancer Drug Des.* **1989**, *4*, 241.
2. Demeunynck, M.; Charmantray, F.; Martelli, A. *Curr. Pharm. Design* **2001**, *7*, 1703.
3. Braña, M. F.; Cacho, M.; Gradillas, A.; de Pascual-Teresa, B.; Ramos, A. *Curr. Pharm. Design* **2001**, *7*, 1745.
4. Robinson, M. J.; Osheroff, N. *Biochemistry* **1990**, *29*, 2511.
5. Gourdie, T. A.; Prakash, A. S.; Denny, W. A. *J. Med. Chem.* **1991**, *34*, 240.
6. Klika, K. D.; Balentová, E.; Bernát, J.; Imrich, J.; Vavrušová, M.; Kleinpeter, E.; Pihlaja, K.; Koch, A. *J. Heterocycl. Chem.* **2006**, *43*, 633.
7. Balentová, E.; Imrich, J.; Bernát, J.; Suchá, L.; Vilková, M.; Prónayová, N.; Kristian, P.; Pihlaja, K.; Klika, K. D. *J. Heterocycl. Chem.* **2006**, *43*, 645.
8. Klika, K. D.; Bernát, J.; Imrich, J.; Chomča, I.; Sillanpää, R.; Pihlaja, K. *J. Org. Chem.* **2001**, *66*, 4416.
9. Kristian, P.; Bernát, J.; Imrich, J.; Danihel, I.; Suchár, G.; Hočová, S.; Bušová, T.; Guspanová, J.; Linden, A. *Molecules* **1996**, *1*, 181.
10. Kristian, P.; Chomča, I.; Bernát, J.; Imrich, J. *Chem. Papers* **1999**, *53*, 49.
11. Kristian, P.; Bernát, J.; Imrich, J.; Sedlák, E.; Alföldi, J.; Čornanič, M. *Heterocycles* **2001**, *55*, 279.
12. Bernát, J.; Chomča, I.; Kristian, P.; Pihlaja, K.; Klika, K. D.; Imrich, J. *Heterocycles* **1999**, *51*, 137.
13. Kristian, P.; Balentová, E.; Bernát, J.; Imrich, J.; Sedlák, E.; Danihel, I.; Böhm, S.; Prónayová, N.; Klika, K. D.; Pihlaja, K.; Baranová, J. *Chem. Pap.* **2004**, *58*, 268.
14. Bernát, J.; Balentová, E.; Kristian, P.; Imrich, J.; Sedlák, E.; Danihel, I.; Böhm, S.; Prónayová, N.; Pihlaja, K.; Klika, K. D. *Coll. Czech. Chem. Commun.* **2004**, *69*, 833.
15. Klika, K. D.; Imrich, J.; Vilková, M.; Bernát, J.; Pihlaja, K. *J. Heterocycl. Chem.* **2006**, *43*, 739.
16. Klika, K. D.; Janovec, L.; Imrich, J.; Suchár, G.; Kristian, P.; Sillanpää, R.; Pihlaja, K. *Eur. J. Org. Chem.* **2002**, 1248.
17. Klika, K. D.; Valtamo, P.; Janovec, L.; Suchár, G.; Kristian, P.; Imrich, J.; Kivelä, H.; Alföldi, J.; Pihlaja, K. *Rapid Commun. Mass Spectrom.* **2004**, *18*, 87.
18. Adcock, B. *Aminoacridines* In *Acridines*, Acheson R. M., Ed. *The Chemistry of Heterocyclic Compounds*, Weissberger, A.; Taylor, E. C., Eds.); J. Wiley: New York, 1973, pp 109.
19. (a) Valters, R. E.; Fülöp, F.; Korbonits, D. *Adv. Heterocycl. Chem.* **1995**, *64*, 251; (b) Valters, R. E.; Fülöp, F.; Korbonits, D. *Adv. Heterocycl. Chem.* **1996**, *66*, 1.
20. See for example: Laatikainen, R.; Niemitz, M.; Weber, U.; Sundelin, J.; Hassinen, T.; Vepsäläinen, J. *J. Magn. Reson. Ser. A* **1996**, *120*, 1. See also: *Peak Research NMR Software*, Perch Solutions Ltd., Kuopio, Finland, 2003 (http://www.perchsolutions.com).
21. For example: (a) de Matos Gomes, E.; Nogueira, E.; Belsley, M. S.; Costa, M. M. R. *Proc. SPIE* **2002**, *4751*, 223; (b) Qiao, X.; Xiao, X.; Wang, X.; Yang, J.; Qiu, Z.; An, L.; Wang,

W.; Mo, Z. *Eur. Polym. J.* **2002**, *38*, 1183; (c) Yang, H.; Yan, X.-h.; Wang, Z.-l.; Cheng, R.-s. *Gao. Xue. Hua. Xue.* **2001**, *22*, 666.

22. Gardner, M. *The New Ambidextrous Universe: Symmetry and Asymmetry from Mirror Reflections to Superstrings*; 3rd Edn., Dover Publications, Inc: Mineola, New York, 2005.

23. In Pasteur's time, magnetic fields were erroneously thought to be intrinsically asymmetric.

24. Tähtinen, P.; Bagno, A.; Klika, K. D.; Pihlaja, K. *J. Am. Chem. Soc.* **2003**, *125*, 4609.

25. Rosling, A.; Klika, K.; Fülöp, F.; Sillanpää, R.; Mattinen, J. *Heterocycles* **1999**, *51*, 2575.

26. Rosling, A.; Klika, K. D.; Fülöp, F.; Sillanpää, R.; Mattinen, J. *Acta Chem. Scand.* **1999**, *53*, 103.

27. Rosling, A.; Hotokka, M.; Klika, K. D.; Fülöp, F.; Sillanpää, R.; Mattinen, J. *Acta Chem. Scand.* **1999**, *53*, 213.

28. Klika, K. D.; Mäki, J.; Sjöholm, R.; Kronberg, L. *Arkivoc* **2006**, (*xii*), 65.

29. Roslund, M. U.; Virta, P.; Klika, K. D. *Org. Lett.* **2004**, *6*, 2673.

30. Nuzillard, J.-M.; Gasmi, G.; Bernassau, J.-M. *J. Magn. Reson. Ser. A* **1993**, *104*, 83.

31. Bennett, A. E.; Rienstra, C. M.; Auger, M.; Lakshmi, K. V.; Griffin, R. G. *J. Chem. Phys.* **1995**, *103*, 6951.

32. (a) Murphy, P. D. *J. Magn. Reson.* **1983**, *52*, 343; (b) Murphy, P. D. *J. Magn. Reson.* **1985**, *62*, 303; (c) Alemany, L. B.; Grant, D. M.; Alger, T. D.; Pugmire, R. J. *J. Am. Chem. Soc.* **1983**, *105*, 6697.

33. Wu, X.; Zilm, K. W. *J. Magn. Reson. Ser. A* **1993**, *102*, 205.

34. Sangill, R.; Rastrup-Andersen, N.; Bildsøe, H.; Jakobsen, H. J.; Nielsen, N. C. *J. Magn. Reson. Ser. A* **1994**, *107*, 67.

35. Sheldrick, G. M. *SHELXS-97. Program for Crystal Structure Solution*, Göttingen 1997.

36. Sheldrick, G. M. *SHELXS-97. Program for Crystal Structure Refinement*, Göttingen 1997.